Article

DNA intercalation facilitates efficient DNA-targeted covalent binding of phenanthriplatin

Ali A. Almaqwashi, Wen Zhou, M. Nabuan Naufer, Imogen A. Riddell, Ömer H. Yilmaz, Stephen J. Lippard, and Mark C. Williams

J. Am. Chem. Soc., **Just Accepted Manuscript** • DOI: 10.1021/jacs.8b10252 • Publication Date (Web): 02 Jan 2019

DNA intercalation facilitates efficient DNA-targeted covalent binding of phenanthriplatin

Ali A. Almaqwashi[1,†], Wen Zhou[3,4,†], M. Nabuan Naufer[2], Imogen A. Riddell[3,5], Ömer H. Yilmaz[4], Stephen J. Lippard[3,4], and Mark C. Williams[2]

[1]Physics Department, King Abdulaziz University, Rabigh, 21911, Saudi Arabia

[2]Department of Physics, Northeastern University, Boston, MA, 02115, USA

[3]Department of Chemistry, Massachusetts Institute of Technology, Cambridge, MA, 02139, USA

[4]David H. Koch Institute for Integrative Cancer Research at MIT, Cambridge, MA 02139, USA

[5]Department of Chemistry, The University of Manchester, Manchester, M13 9PL, UK

[†]These authors contributed equally

¶Corresponding Author:

Mark C. Williams
Northeastern University
Department of Physics
Boston, MA 02115
Phone: 617-373-7323
Email: mark@northeastern.edu

Abstract

Phenanthriplatin, a monofunctional anticancer agent derived from cisplatin, shows significantly enhanced DNA covalent binding activity compared to its parent complex. To understand the underlying molecular mechanism, we use single molecule studies with optical tweezers to probe the kinetics of DNA-phenanthriplatin binding as well as DNA binding to several control complexes. The time-dependent extension of single λ-DNA molecules were monitored at constant applied forces and compound concentrations, followed by rinsing with a compound-free solution. DNA-phenanthriplatin association consisted of fast and reversible DNA lengthening with time constant τ ~10 s, followed by slow and irreversible DNA elongation that reaches equilibrium in ~30 min. In contrast, only reversible fast DNA elongation occurs for its stereoisomer trans-phenanthriplatin, suggesting that the distinct two-rate kinetics of phenanthriplatin is sensitive to the geometric conformation of the complex. Furthermore, no DNA unwinding is observed for pyriplatin, in which the phenanthridine ligand of phenanthriplatin is replaced by the smaller pyridine molecule, indicating that the size of the aromatic group is responsible for the rapid DNA elongation. These findings suggest that the mechanism of binding of phenanthriplatin to DNA

involves rapid, partial intercalation of the phenanthridine ring followed by slower substitution of the adjacent chloride ligand by, most likely, the N7 atom of a purine base. The cis isomer affords the proper stereochemistry at the metal center to facilitate essentially irreversible DNA covalent binding, a geometric advantage not afforded by *trans* phenanthriplatin. This study demonstrates that reversible DNA intercalation can be employed to provide a robust transition state that is efficiently converted to an irreversible DNA-Pt bound state.

INTRODUCTION

It was estimated in 2017 that ~1.7 million new cancer cases would be diagnosed in the US [1], and by 2030, it is expected globally to hit 22 million new cases per year.[2-3] The synthesis and evaluation of new anti-cancer therapeutics is sought in urgent demand to overcome persisting disadvantages of current agents, including side-effects, lower effectiveness against certain cancers, and inherent or acquired resistance.[4-5] Clinically used platinum-based drugs including cisplatin, carboplatin, and oxaliplatin are treating various cancers such as endocrine-related testicular and ovarian carcinomas, lung cancers, myelomas, and lymphomas.[6] Despite their relative success, developing non-classical platinum complexes that operate via mechanisms of action distinct from those of the approved drugs is of great importance.[7]

One strategy for developing such non-classical platinum complexes has been to design target compounds that violate the traditional structure–activity relationships established in the 1970's.[8] Phenanthriplatin, a potent monofunctional compound, was synthesized by replacing one of the chloride ligands of cisplatin with a phenanthridine group.[9] This compound is 7 to 40 times more active than cisplatin and displays a spectrum of anti-cancer activity that differs significantly from that of any other platinum-based anti-cancer agent in the National Cancer Institute database.[9] Phenanthriplatin exhibits higher effectiveness on all tested cell lines compared to other anticancer agents evaluated based on previously reported IC_{50} values by *Zhou et al*, [10] represented in Fig.1. These results reveal an order of magnitude lower IC_{50} values for phenanthriplatin across all cell lines. Interestingly, the structurally analogous complex, pyriplatin, is much less potent than that of cisplatin.[11] Further, the geometric isomer, a *trans*-DDP-based phenanthriplatin, was also synthesized (Figure 2A), yet its anti-cancer activity is also significantly less than that of phenanthriplatin.[10]

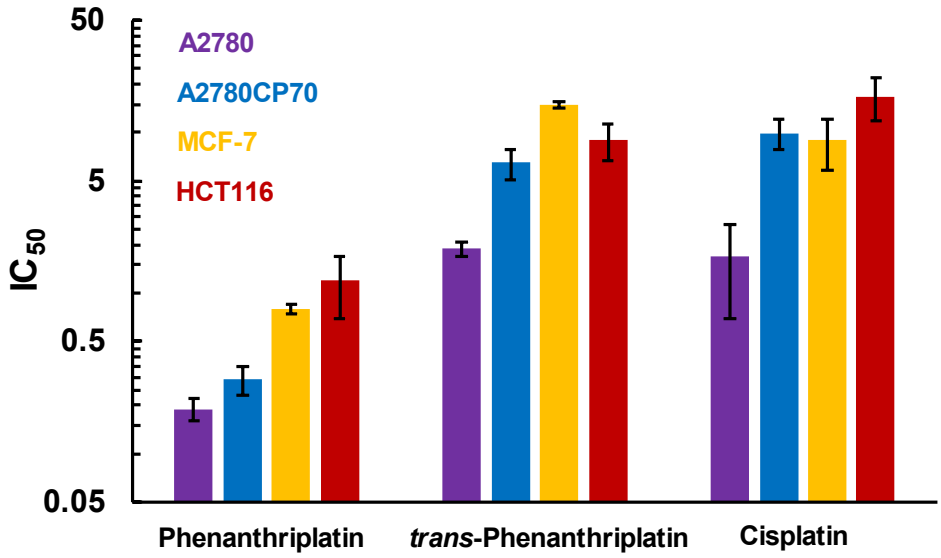

Fig.1 IC_{50} values previously reported by *Zhou et al*[10] for phenanthriplatin, *trans*-phenanthriplatin, and cisplatin examined in various cell lines, represented in color-coded bars.

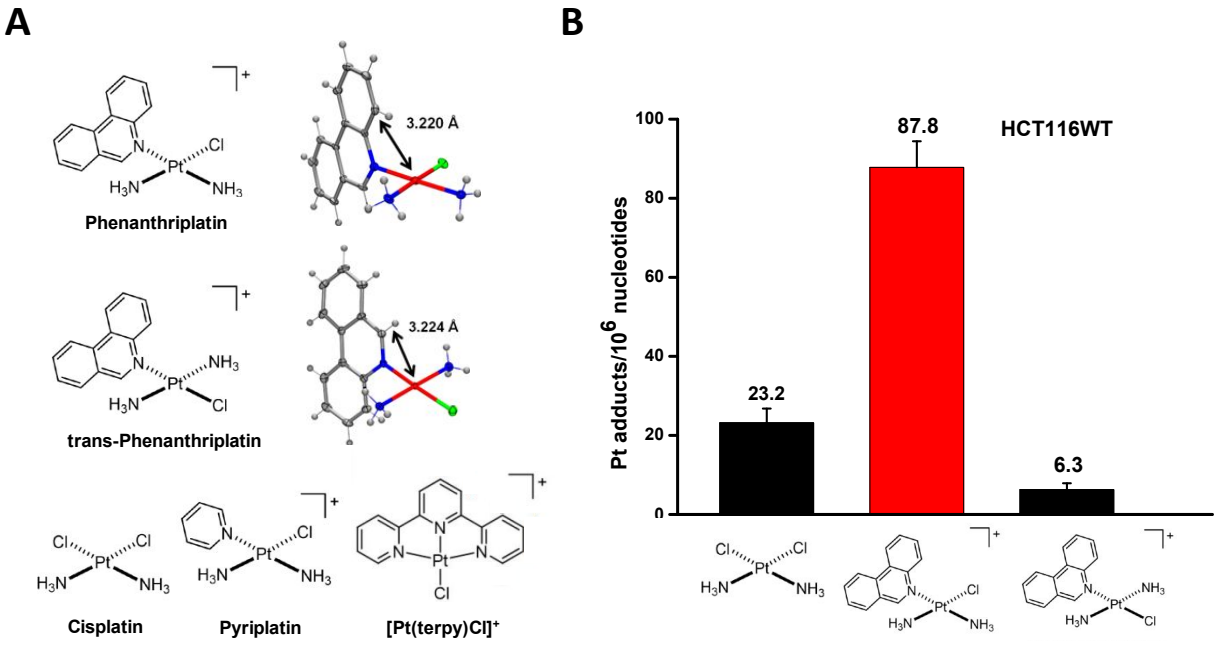

Fig. 2 A) The structures of platinum-based anti-cancer agents: phenanthriplatin, *trans*-phenanthriplatin, cisplatin, pyriplatin, and $[Pt(terpy)Cl]^+$, respectively. The solid-state structures of phenanthriplatin and *trans*-phenanthriplatin are also provided, the dihedral angles are 88.88°(20) for phenanthriplatin and 67.157°(169) for *trans*-phenanthriplatin. B) Bars indicate platinum adducts per million nucleotides measured for DNA extracted from cell line HCT116WT after

being treated and incubated with cisplatin, phenanthriplatin, or *trans*-phenanthriplatin, respectively. Values reflect the mean and standard deviation of results from three separate experiments.

Although equilibrium and structural studies may reveal characteristics of the DNA-phenanthriplatin covalent adduct, the preceding transition states traversed during the DNA platination step(s) are not known. We aimed to identify the origin of the differential anticancer activity observed for the two isomers. To understand the mechanism that leads to the observed enhanced covalent binding of phenanthriplatin to DNA, here we probe the detailed kinetics of phenanthriplatin binding by single molecule DNA stretching experiments. Because single molecule stretching is very sensitive to DNA unwinding, by even weakly intercalating small molecules, this method is an excellent probe of DNA deformation that occurs prior to covalent modification.[12] We show that phenanthriplatin binds DNA in a two-step process in which rapid unwinding of DNA is followed by slow covalent modification. Surprisingly, although the phenanthriplatin stereoisomer *trans*-phenanthriplatin rapidly unwinds DNA, it does not show significant covalent DNA binding, and the initial DNA-bound state is fully reversible. Therefore, *trans*-phenanthriplatin is a much less efficient DNA modification agent. Thus, the orientation of the leaving group, a chloride ion, in phenanthriplatin appears to be optimal to take advantage of the initially intercalative DNA binding to facilitate subsequent robust covalent binding.

MATERIALS AND METHODS

Platinum compounds

Stock solutions of platinum compounds were prepared in PBS. Cisplatin was purchased from Strem Chemicals. The platinum compounds phenanthriplatin, *trans*-phenanthriplatin, pyriplatin, and $[Pt(terpy)Cl]^+$ were synthesized as described elsewhere[9-10, 13] and their identities were confirmed by ^1H NMR spectroscopic measurements (see Supporting Information).

DNA platination measurements

For these studies, 2 million cells of each tested cell line were seeded on 100 mm × 20 mm petri dishes and incubated for 24 h at 37 °C. These cells were then treated with the platinum compounds (10 μM) for 5 h at 37 °C. Afterward, fresh medium was added, followed by an additional 16 h of incubation at 37 °C. The medium was then removed and the cells were washed with PBS (2 x 2 mL), harvested by trypsinization (1 mL), and washed with 2 mL of PBS twice. Solutions containing cells were centrifuged at 1500 rpm for 5 min at 4 °C. The cell pellets were suspended in DNAzol (1 mL, genomic DNA isolation reagent, MRC). The DNA was precipitated with pure ethanol (0.5 mL), washed with 75% ethanol (0.75 mL × 3), and re-dissolved in 0.4 mL of 8 mM NaOH. The DNA concentration was determined by NanoDrop Spectrophotometer (Thermo Fisher Scientific) and the platinum content was quantitated by graphite furnace atomic absorption spectroscopy.

Cell line and cell line culture

Human colorectal carcinoma HCT116 was incubated at 37 °C in 5% CO_2 and grown in DMEM medium supplemented with 10% fetal bovine serum and 1% penicillin/streptomycin. Cells were passaged every 3 to 4 days and restarted from the frozen stock upon reaching passage number 25.

Single molecule DNA stretching measurements

Single molecule experiments utilized dual-beam optical tweezers (laser wavelength 830 nm). Each experiment was conducted with a single bacteriophage λ-DNA (contour length 16.5 μm), biotin-labeled on opposite strands and attached to two streptavidin-coated polystyrene beads (~5.6 μm). One bead was held in an optical trap and another bead was held by a micropipette mobilized by a piezoelectric positioner (±5 nm) to maintain a fixed stretching force (±1 pN) on the DNA molecule. The free DNA stretching curve was obtained (Fig. 3A, black data points) at a pulling rate of ~200 nm/s. The DNA molecule was then maintained at a desired force in the presence of the compound (association, Fig. 3A, purple data points) and subsequently in the absence of free compounds in the solution (dissociation, Fig. 3A, blue data points), registering the temporal change in extension via a force-feedback system tracing DNA extension as the compound dissociated. The force feedback module responds to any sudden force change by displacing the micropipette to maintain the assigned force, while acquiring data at time intervals as fast as 10 ms. The subsequent DNA stretching curve was obtained in compound-free buffer at a pulling rate of ~200 nm/s (Fig. 3A orange data points). The experiments were conducted with a 100 μl flow cell chamber. Both association and dissociation experiments were measured under a continuous flow (~2 μl/s) of compound solution and compound-free buffer, respectively, to ensure constant compound concentration in association experiments, and to rinse out residual compound during dissociation. The measurements were obtained on at least three DNA molecules for each averaged data point. All experiments were conducted at 21 ºC in 10 mM Tris buffer, 100 mM NaCl, and at pH 8.

Molecular docking

To visualize and assess the proposed molecular mechanism, molecular docking of phenanthriplatin and *trans*-phenanthriplatin to the Dickerson dodecamer DNA duplex d(CpGpCpGpApApTpTpCpGpCpG)[14] was performed with AutoDock [Scripps Research Institute].[15] The resulting docking conformations to the minor and major grooves were ranked based on energy minimization as well as access to intercalation and/or covalent binding. For phenanthriplatin, the docking conformation was further used to assemble the phenanthridine moiety into the intermediate intercalation coordinates and the final intercalated and covalently bonded state. The assembled structures were sterically minimized by utilizing Chimera [University of California-San Francisco][16-17] and the initial coordinates of the DNA duplex, phenanthriplatin, and *trans*-phenanthriplatin were obtained from published crystal structures.[10, 14]

RESULTS

Force spectroscopy probes DNA intercalation and subsequent modification by phenanthriplatin

DNA platination experiments conducted in this study reveal that phenanthriplatin has a much greater number of Pt-DNA adducts relative to those of cisplatin and *trans*-phenanthriplatin, as shown in Fig. 2B for cell line HCT116WT, which is also consistent with previous observations.[9, 18-19] Interestingly, the stereoisomer *trans*-phenanthriplatin did not exhibit such enhanced DNA covalent binding, a significant observation that was thoroughly examined in the single molecule approach, as described below.

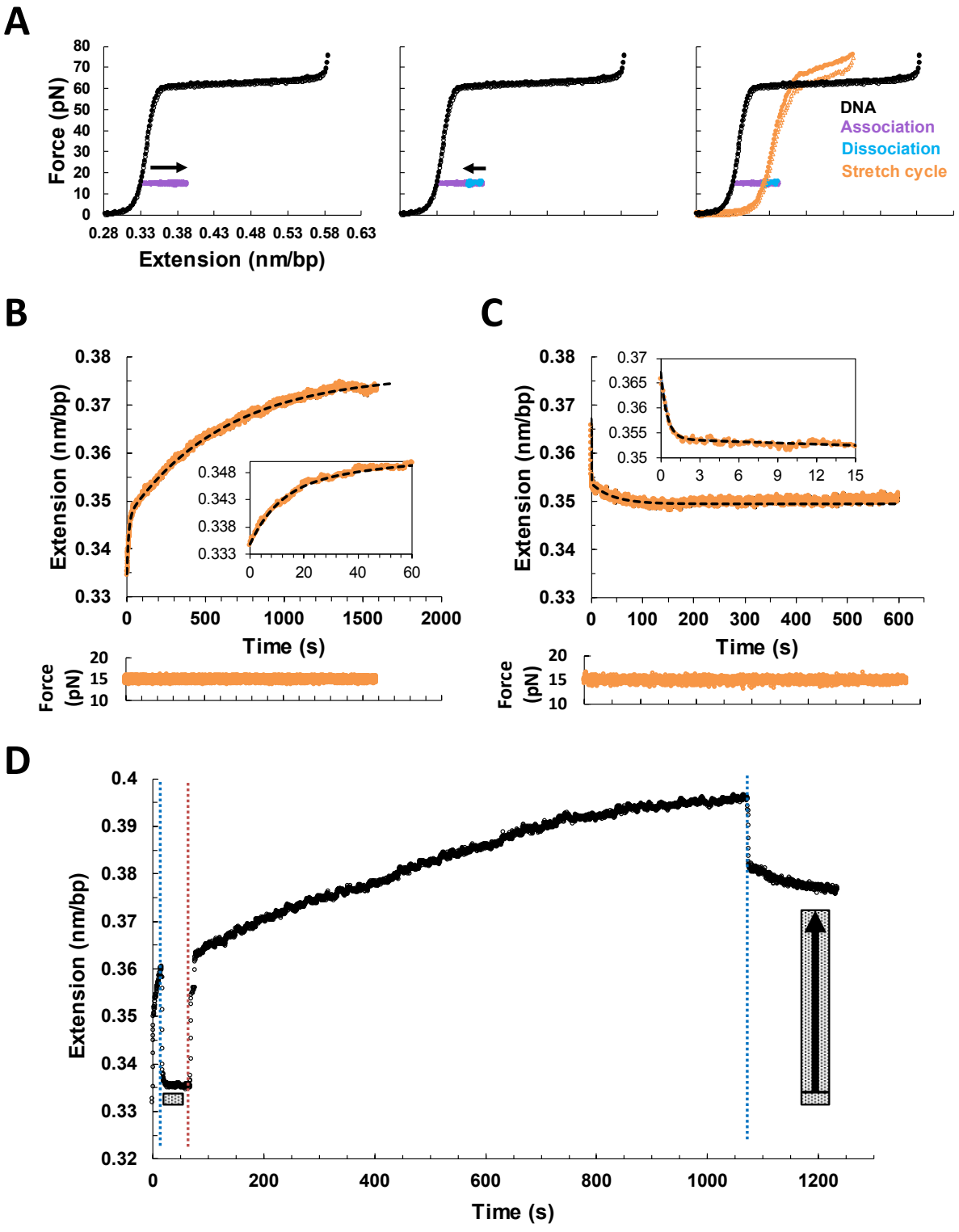

Fig. 3 Single molecule DNA stretching measurements of DNA-phenanthriplatin. For constant force measurements, a single DNA molecule is held at 15 pN, followed by association in 3 μM compound concentration and dissociation in compound-free buffer. A) Force-extension measurements at constant force. The stretch and release of DNA only is

shown as black symbols. Subsequent DNA-phenanthriplatin association data at constant force is shown in purple (left graph), followed by DNA-phenanthriplatin dissociation data in blue (middle graph). The orange data points show the DNA stretch and release force-extension curves in compound-free buffer (right graph) after intercalation and covalent binding has occurred. For force-extension curves, solid circles represent stretch data points and open triangles represent release data points. (B) DNA-phenanthriplatin association kinetics (C) DNA-phenanthriplatin dissociation kinetics, data points displayed in orange, double exponential fits shown with dashed black lines, the association fitted to time constants of $\tau_{on,1}$ =11.6 ±2 s and $\tau_{on,2}$ =625 ±10 s, and the partial dissociation fitted to time constants of $\tau_{off,1}$ =0.48 ± 0.18 s and $\tau_{off,2}$ =41 ± 14 s. Insets show the data and fits at short timescales and the constant force data is below the time axis label. D) The association and dissociation of DNA-phenanthriplatin at short (~15 s) and long (~1000 s) timescales (black data points), where an arrow represents the change in irreversible DNA elongation. Blue dashed lines denote switching to compound-free buffer, and the orange dashed line denotes switching back to 3 μM concentration of phenanthriplatin. Shaded bars illustrate the magnitude of permanent DNA modification. The time constants and fits shown in this figure are for the specific examples shown, with uncertainties determined by the error in the fit. Average values are reported in the text.

To investigate phenanthriplatin covalent binding to DNA, single-molecule force spectroscopy with optical tweezers was utilized to probe DNA-phenanthriplatin binding in real time. DNA extension was traced for tens of minutes, as shown in Fig. 3B, at a constant applied force of 15 pN and a compound concentration of 3 μM. The results show that phenanthriplatin association results in two phases of DNA elongation: fast elongation, with a time constant of $\tau_{on,1}$ =10 ± 2 s, followed by slow elongation, with time constant $\tau_{on,2}$ =639 ± 90 s. The reported time constants represent averages for three measurements, with uncertainty presented as standard error of the mean. One example with its fit is shown in Fig. 3B. The fast elongation resembles that observed previously for other compounds containing phenanthridine, in which weak DNA intercalation was enhanced by force, allowing DNA force-dependent and zero force DNA intercalation affinity to be measured.[12, 20] After reaching the equilibrium extension, the free compound in the solution was rinsed, as illustrated in Fig. 3C. The elongation of the compound-bound DNA molecule is only partially recovered within the timescale of our experiments (~10 s) upon the dissociation of the bound compounds. The recovery of the DNA elongation occurs in a biphasic manner, in which a fast dissociation of $\tau_{off,1}$ =0.54 ± 0.05 s is followed by a slow dissociation of $\tau_{off,2}$ =50 ± 20 s of the bound-compounds (averages for three measurements). The subsequent force-extension profiles in the absence of free compounds (Fig. 3A orange data points) confirm that a fraction of the DNA molecule is permanently elongated owing to bound phenanthriplatin, indicating covalent modification.

The progression of permanent DNA elongation was examined by measuring the dissociation kinetics at two different timescales (~15 and 1000 s) upon incubation with the compound. Fig. 3D shows the fractions of permanent DNA-phenanthriplatin binding after ~15 s and 1000 s of DNA elongation due to compound binding. After 15 s, very little DNA is permanently modified, as shown by the shaded bar. Re-incubation of the same DNA molecule with phenanthriplatin yields a much higher fraction of permanently modified DNA, as shown by the grey bar at ~1200 s. These results reveal that the fast phase DNA

elongation by phenanthriplatin is mostly reversible and is consistent with the previously studied simple intercalators,[12, 20-21] whereas the slow phase DNA-phenanthriplatin binding represents covalent modification.

Control platinum-based agents do not permanently lengthen DNA

DNA binding to other platinum-based agents was investigated as a control to identify the contribution of the phenanthridine moiety to DNA lengthening and enhanced DNA covalent binding. The stereoisomer *trans*-phenanthriplatin has the phenanthridine moiety positioned trans to the leaving chloride ion leaving group (Fig. 2A). In contrast to phenanthriplatin, this stereoisomer does not manifest a distinctively slow phase of association (Fig. 4A) under similar experimental conditions (F=15 pN, 3 μM compound). After fitting the data to a sum of two exponential functions, the kinetics of *trans*-phenanthriplatin association yielded two average time constants $\tau_{on,1}$ =2.3 ±1 s and $\tau_{on,2}$ =8 ±2 s, comparable to the fast phase time constant observed for phenanthriplatin.

In compound-free buffer, the dissociation of DNA-compound complex fully recovers the free DNA extension (τ = 1.14 ±0.1 s). Although the subsequent force-extension cycles (see supplementary Figure S5) show permanent DNA force-extension curve changes that are consistent with covalent modification, a significant elongation of the DNA is not observed. Thus, this covalent modification is presumably due to binding that is not facilitated through DNA intercalation. This suggests that the configuration of the phenanthridine moiety relative to the chloride ligand is critical to enhance the formation of the covalent bond because, in contrast to phenanthriplatin, the phenanthridine moiety of the stereoisomer resides on the opposite side of the leaving chloride group.

We also examined platinum-based agents with different aromatic functionality. In particular, terpyriplatin, a known DNA intercalator,[13] has the terpyridine moiety configured oppositely to the chloride ligand, similar to trans-phenanthriplatin. Fig. 4B shows that $[Pt(terpy)Cl]^+$ also exhibits DNA intercalation that is not simultaneous to DNA-compound covalent binding (on a timescale of 1000 s), as all of the observed intercalative binding is reversible. Although covalent binding likely occurs with $[Pt(terpy)Cl]^+$, because the intercalation and covalent binding are not simultaneous, the covalent binding does not result in DNA lengthening and is therefore not observed in our study. This also suggests that intercalation does not enhance covalent binding for $[Pt(terpy)Cl]^+$. Pyriplatin is an analogue to phenanthriplatin but the phenanthridine moiety is replaced by a smaller aromatic pyridine moiety. Fig. 4C shows that pyriplatin does not induce significant DNA elongation, even at two orders of magnitude higher concentration (~300 μM). As a negative control DNA-cisplatin binding is tested. As expected,[22] cisplatin did not induce DNA elongation, instead, we observed a slow rate of DNA compaction, as illustrated in Fig. 4D. This result is consistent with previous single molecule measurements of DNA modification by cisplatin[23-24] as well as earlier observations that cisplatin caused DNA shortening in the absence of force.[22]

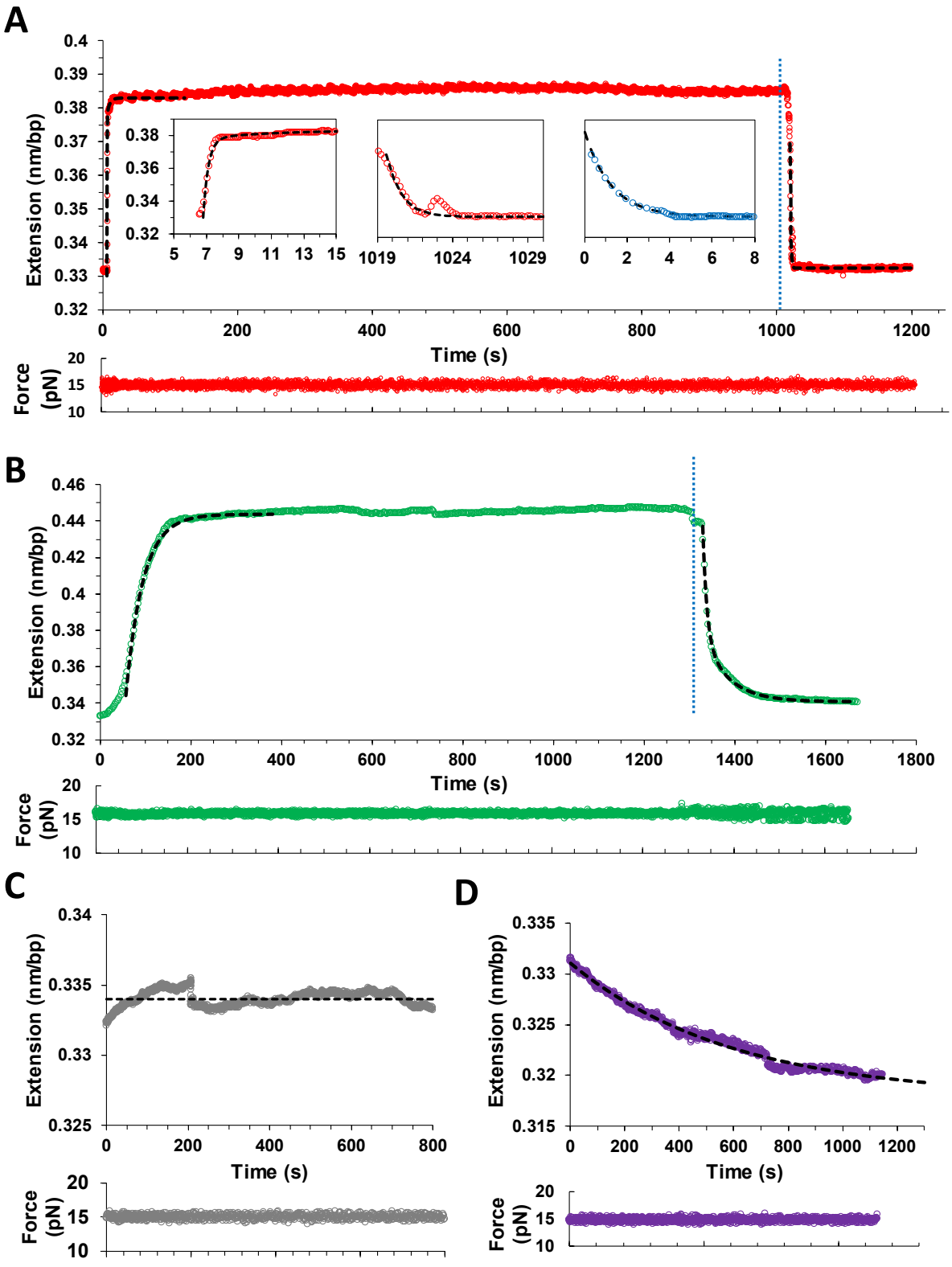
A
Extension (nm/bp)
Time (s)
Force (pN)
B
Extension (nm/bp)
Time (s)
Force (pN)
C
Extension (nm/bp)
Time (s)
Force (pN)
D
Extension (nm/bp)
Time (s)
Force (pN)

Fig. 4 Single molecule DNA stretching measurements of DNA-compound binding, with all the experiments conducted at a constant force of 15 pN. A) DNA-*trans*-phenanthriplatin association, in 3 μM compound concentration, and dissociation in compound-free buffer. The blue dashed line denotes switching to compound-free buffer, the DNA extension data points are shown in red, and the black dashed lines are fits, with the association fitted with double exponential of time constants $\tau_{on,1}$ =0.32 ±0.05 s and $\tau_{on,2}$ =4.1 ±1.4 s, and the dissociation fitted with single exponential of time constant τ_{off} =1.2 ± 0.1 s. Insets show the data and fits at short timescales. The relaxation curve for this dataset contains an artifact not reproduced in other datasets (middle inset, data points in red), so we also present the average of three relaxation curves in the inset (blue data points). The time axis is reset to zero to allow for time offset in the averaging process. B) DNA- $[Pt(terpy)Cl]^+$ association at 3 μM compound concentration, and dissociation in compound-free buffer. The blue dashed line is for switching to compound-free buffer, the DNA extension data points are in green, and black dashed lines are used for the fits. The association and dissociation are fitted with double exponentials, and the time constants for association are $\tau_{on,1}$ =36 ±1 s and $\tau_{on,2}$ =50 ±4 s; the time constants for dissociation are $\tau_{off,1}$ =9 ±0.5 s and $\tau_{off,2}$ =56 ±3 s. C) DNA-pyriplatin experiment, at 300 μM compound concentration and a constant stretching force of 15 pN. DNA extension data points are in gray, and the black dashed line denotes the average DNA extension. which does not show a significant DNA elongation. D) DNA-cisplatin experiment, at 30 μM compound concentration. The purple data points are for DNA extension, and the black dashed line for the fit, the decrease in extension indicating DNA compaction fitted to a single exponential yielding a time constant τ =588 ±40 s. The constant force data is below the time axis label. The time constants and fits depicted in this figure are for the specific examples shown, with uncertainties determined by the error in the fit. Average values are reported in the text.

To understand the role of force in determining the two-step reaction rate for phenanthriplatin, we also varied the applied constant force and measured the resulting binding kinetics. Constant force measurements obtained at 10 pN and are presented in Figure S6. The initial fast time constant was $\tau_{on,1}$ (15 pN) =10 ± 2 s at 15 pN and this value changed to $\tau_{on,1}$ (11 pN) =14 ± 5 s. The second, slow phase time constant decreased from 639± 90 s at 15 pN to 866± 97 s at 11 pN. Although both time constants depend on force, we show below that the force dependence is primarily due to the initial intercalation step.

DISCUSSION

DNA elongation by platinum-based agents is linked to the aromatic group

The present observations reveal that platinum-based agents of similar positive charge can differ in their ability to elongate DNA based on the nature of their aromatic group. We find that pyriplatin, which has a single aromatic heterocyclic ligand, does not elongate DNA, whereas phenanthriplatin and *trans*-phenanthriplatin elongate DNA in a manner similar to that of $[Pt(terpy)Cl]^+$, the first metallointercalator identified (Fig. 2A).[13, 25-26] This result indicates that the phenanthridine moiety is intimately involved in DNA elongation by phenanthriplatin and *trans*-phenanthriplatin. Moreover, the reversible DNA elongation rates for phenanthriplatin and *trans*-phenanthriplatin are comparable to those observed for previously

reported DNA intercalators, including examples of complexes that exhibit one or two phase dissociation kinetics.[12, 20-21, 27-30] Notably, the measured DNA equilibrium elongation by *trans*-phenanthriplatin binding provides an insightful estimate of the force-dependent equilibrium dissociation constant K_d. For an exponential force dependence of DNA elongation[12, 20] (see Supporting Information, section III), we estimate the zero-force equilibrium dissociation constant K_d to be 10 to 30 μM, which is consistent with previously reported values of K_d for DNA intercalation by phenanthridinium derivatives.[31] That this estimated affinity is an order of magnitude weaker than DNA intercalation affinity by the classical intercalator ethidium[20] most likely reflects the fact that coordination of the phenanthridine to platinum in phenanthriplatin block full intercalative insertion into the duplex; such partial intercalation would lead to a weaker binding constant and probably facilitate the subsequent covalent binding step. These findings demonstrate that the reversible phase of DNA elongation by phenanthriplatin includes, in addition to DNA unwinding, a weak-affinity of partial intercalation by the phenanthridine moiety. The results also suggest that single molecule stretching could be used to probe other metal anticancer complexes that also contain potential intercalating moieties [32].

Detailed analysis of the rates of DNA elongation and decay for phenanthriplatin and *trans*-phenanthriplatin are presented in the Supporting Information (section V). Analysis of the force-dependent kinetics of phenanthriplatin association shows that the reaction can be fully modelled as a two-step reaction consisting of an intercalation step followed by a covalent binding step. Although both observed elongation rates exhibit a weak dependence on force, separate determination of the fundamental reaction rates reveals an initial force-dependent and concentration-dependent intercalation rate k_1 followed by a force-independent covalent binding rate $k_2 = 5 \pm 2 \times 10^{-3}$ s^{-1}. Both compounds exhibit decay kinetics that are comparable to previously reported dissociation rates from a deformed intercalated DNA base pair.[27, 29-30] This is also consistent with a two-step reaction, in which only dissociation from the intercalated state is observed.

Stereoselective DNA deformation by phenanthriplatin enhances the covalent binding

Reversible DNA elongation is observed for both phenanthriplatin and *trans*-phenanthriplatin, but only phenanthriplatin exhibits a subsequent slow and irreversible increase of the DNA duplex length. From equilibrium and kinetics analyses, we propose that this stereoselective second intermediate elongated state is an optimized conformation that affects subsequent formation of covalent adducts with the N7 of purine bases.[33-34] A clear distinction is thus observed in the proposed mechanism of action of phenanthriplatin and its geometric isomer *trans*-phenanthriplatin (Fig 5). Molecular docking studies indicate that initial DNA groove binding for *trans*-phenanthriplatin (Fig. 5A) can support either covalent bond formation (major groove) or intercalation (minor groove). In contrast, for phenanthriplatin covalent bond formation can occur simultaneously with partial intercalation of the phenanthridine ring at the nearest neighbor base pair (Fig 5B, C, D and E). DNA intercalation by *trans*-phenanthriplatin is thus a

competitive binding mode that minimizes covalent bond formation on the timescale of tens of minutes. In contrast, DNA-phenanthriplatin covalent bonding is enhanced by DNA deformation (Fig 5C) that favorably drives the energy landscape pathways toward covalent bond formation. The result is a robust stereo-sensitive mechanism that employs a controllable intermediate DNA deformation state to optimize the efficiency of the DNA-targeted therapeutics.

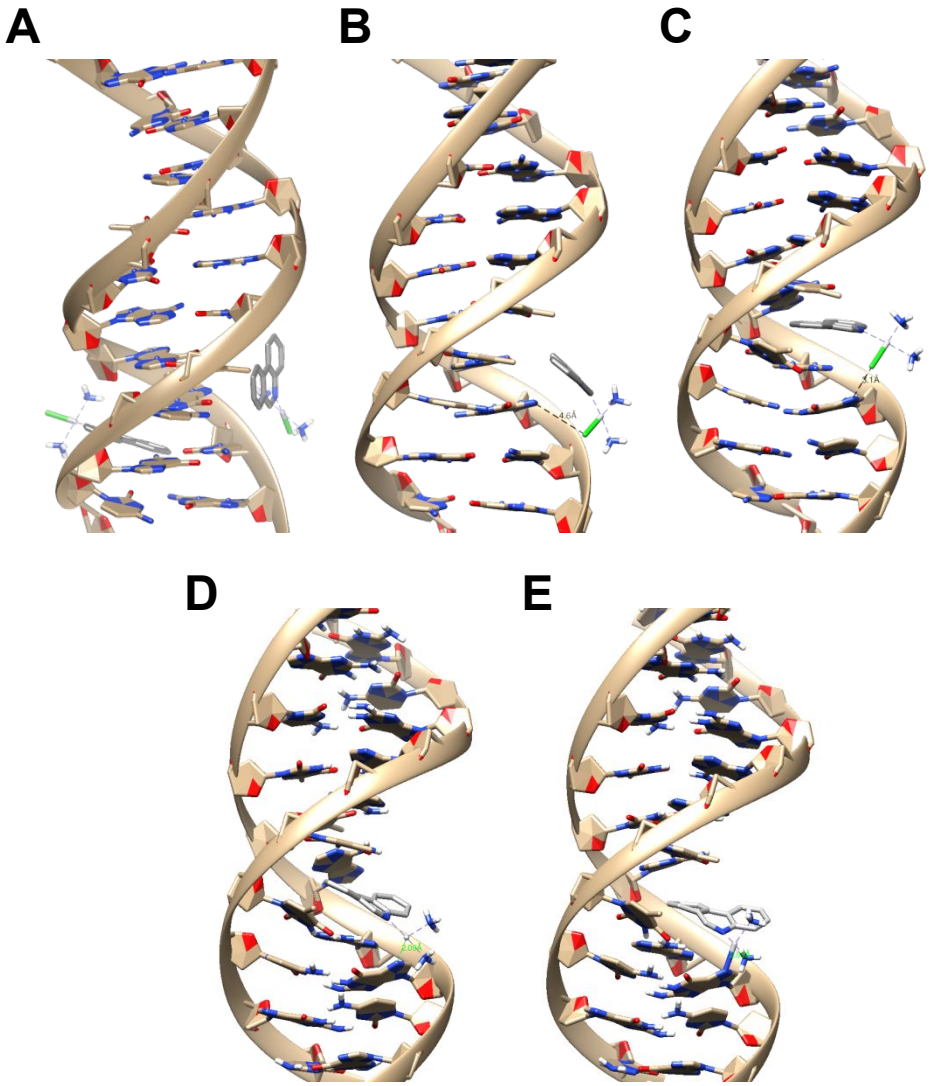

Fig. 5 A) Illustration of minor (left) and major (right) groove binding conformations for *trans*-phenanthriplatin that supports either intercalation or covalent binding, respectively. B) Illustration of a major groove binding conformation for phenanthriplatin that supports both partial intercalation and covalent binding, simultaneously. C) Illustration of the proposed intermediate intercalated state which further positions phenanthriplatin in proximity to the covalent bond coordination site, the N7 atom of a G base, as the phenanthridine moiety intercalates the next nearest neighbour base pair. D&E) Illustration of the proposed final state in which phenanthriplatin is covalently bonded to DNA by

substitution of the chloride ligand by N7 atom of a purine base while simultaneously intercalating the next nearest neighbour base pair. The conformations and illustrations were obtained as detailed in Materials and Methods.

In conclusion, we discovered that the choice of aromatic moiety as well as the stereochemical arrangement of the ligands in non-classical monofunctional platinum anticancer agents critically affects the initial association of these complexes with duplex DNA and, consequently, alters the frequency and rate of covalent adduct formation. For phenanthriplatin the orientation of the labile leaving ligand and the intercalating moiety are optimally arranged to promote formation of irreversible covalent Pt-DNA adducts. In contrast, intercalation of the stereoisomer *trans*-phenanthriplatin inhibits covalent bond formation. These design criteria should further aid our development of non-classical agents having the potential to treat cancers that currently do not respond well to existing platinum compounds including cisplatin and oxaliplatin. Specifically, development of potential anticancer drugs that target the DNA duplex via multiple binding modes, such as intercalation and covalent bonding, may provide optimal binding kinetics and/or affinity to improve the drug efficacy.

ACKNOWLEDGEMENT

FUNDING

This work was supported by NSF grant MCB-1817712 to MCW, NIH grant CA034992 to SJL, and as NIH grants AG045144 and CA211184 to ÖHY.

Supporting Information:

This material is available free of charge via the Internet at http://pubs.acs.org.

I. Examination of ^{1}H NMR spectra for small molecules synthesized in this study.

II. Stretch-release cycle after DNA-drug binding by phenanthriplatin and *trans*-phenanthriplatin

III. Single molecule DNA measurements of DNA-phenanthriplatin at 11 pN constant force.

IV. Estimating the equilibrium dissociation constant from the measured kinetics

V. Kinetics analysis of DNA-phenanthriplatin binding

REFERENCES

1. Siegel, R. L.; Miller, K. D.; Jemal, A., Cancer Statistics, 2017. *CA Cancer J Clin* **2017,** *67* (1), 7-30.

2. Bray, F.; Jemal, A.; Grey, N.; Ferlay, J.; Forman, D., Global cancer transitions according to the Human Development Index (2008–2030): a population-based study. *The Lancet Oncology* **2012,** *13* (8), 790-801.

3. Stewart, W. B.; Wild, P. C.; International Agency for Research on, C., *World Cancer Report 2014*. IARC: Geneva, SWITZERLAND, 2014.

4. Cheung-Ong, K.; Giaever, G.; Nislow, C., DNA-damaging agents in cancer chemotherapy: serendipity and chemical biology. *Chem Biol* **2013,** *20* (5), 648-59.

5. Ruggiero, A.; Trombatore, G.; Triarico, S.; Arena, R.; Ferrara, P.; Scalzone, M.; Pierri, F.; Riccardi, R., Platinum compounds in children with cancer: toxicity and clinical management. *Anticancer Drugs* **2013,** *24* (10), 1007-19.

6. Apps, M. G.; Choi, E. H. Y.; Wheate, N. J., The state-of-play and future of platinum drugs. *Endocrine-Related Cancer* **2015,** *22* (4), R219-R233.

7. Johnstone, T. C.; Suntharalingam, K.; Lippard, S. J., The Next Generation of Platinum Drugs: Targeted Pt(II) Agents, Nanoparticle Delivery, and Pt(IV) Prodrugs. *Chem. Rev.* **2016,** *116* (5), 3436-3486.

8. Hambley, T. W., The influence of structure on the activity and toxicity of Pt anti-cancer drugs. *Coord. Chem. Rev.* **1997,** *166*, 181-223.

9. Park, G. Y.; Wilson, J. J.; Song, Y.; Lippard, S. J., Phenanthriplatin, a monofunctional DNA-binding platinum anticancer drug candidate with unusual potency and cellular activity profile. *Proc Natl Acad Sci U S A* **2012,** *109* (30), 11987-11992.

10. Zhou, W.; Almeqdadi, M.; Xifaras, M. E.; Riddell, I. A.; Yilmaz, O. H.; Lippard, S. J., The effect of geometric isomerism on the anticancer activity of the monofunctional platinum complex trans-[Pt(NH3)2(phenanthridine)Cl]NO3. *Chem Commun* **2018,** *54* (22), 2788-2791.

11. Lovejoy, K. S.; Serova, M.; Bieche, I.; Emami, S.; D'Incalci, M.; Broggini, M.; Erba, E.; Gespach, C.; Cvitkovic, E.; Faivre, S.; Raymond, E.; Lippard, S. J., Spectrum of Cellular Responses to Pyriplatin, a Monofunctional Cationic Antineoplastic Platinum(II) Compound, in Human Cancer Cells. *Mol Cancer Ther.* **2011,** *10* (9), 1709-1719.

12. Almaqwashi, A. A.; Paramanathan, T.; Rouzina, I.; Williams, M. C., Mechanisms of small molecule-DNA interactions probed by single-molecule force spectroscopy. *Nucleic Acids Res* **2016,** *44* (9), 3971-88.

13. Jennette, K. W.; Lippard, S. J.; Vassiliades, G. A.; Bauer, W. R., Metallointercalation reagents. 2-hydroxyethanethiolato(2,2',2'-terpyridine)-platinum(II) monocation binds strongly to DNA by intercalation. *Proc Natl Acad Sci U S A* **1974,** *71* (10), 3839-43.

14. Drew, H. R.; Wing, R. M.; Takano, T.; Broka, C.; Tanaka, S.; Itakura, K.; Dickerson, R. E., Structure of a B-DNA dodecamer: conformation and dynamics. *Proc Natl Acad Sci U S A* **1981,** *78* (4), 2179-83.

15. Morris, G. M.; Huey, R.; Lindstrom, W.; Sanner, M. F.; Belew, R. K.; Goodsell, D. S.; Olson, A. J., AutoDock4 and AutoDockTools4: Automated docking with selective receptor flexibility. *J Comput Chem* **2009,** *30* (16), 2785-91.

16. Pettersen, E. F.; Goddard, T. D.; Huang, C. C.; Couch, G. S.; Greenblatt, D. M.; Meng, E. C.; Ferrin, T. E., UCSF Chimera--a visualization system for exploratory research and analysis. *J Comput Chem* **2004,** *25* (13), 1605-12.

17. Wang, J.; Wang, W.; Kollman, P. A.; Case, D. A., Automatic atom type and bond type perception in molecular mechanical calculations. *J Mol Graph Model* **2006,** *25* (2), 247-60.

18. Kellinger, M. W.; Park, G. Y.; Chong, J.; Lippard, S. J.; Wang, D., Effect of a monofunctional phenanthriplatin-DNA adduct on RNA polymerase II transcriptional fidelity and translesion synthesis. *J Am Chem Soc* **2013,** *135* (35), 13054-61.

19. Riddell, I. A.; Agama, K.; Park, G. Y.; Pommier, Y.; Lippard, S. J., Phenanthriplatin Acts As a Covalent Poison of Topoisomerase II Cleavage Complexes. *ACS Chem Biol* **2016,** *11* (11), 2996-3001.

20. Vladescu, I. D.; McCauley, M. J.; Nunez, M. E.; Rouzina, I.; Williams, M. C., Quantifying force-dependent and zero-force DNA intercalation by single-molecule stretching. *Nat. Methods* **2007,** *4*, 517-522.

21. Biebricher, A. S.; Heller, I.; Roijmans, R. F.; Hoekstra, T. P.; Peterman, E. J.; Wuite, G. J., The impact of DNA intercalators on DNA and DNA-processing enzymes elucidated through force-dependent binding kinetics. *Nat Commun* **2015,** *6*, 7304.

22. Cohen, G. L.; Bauer, W. R.; Barton, J. K.; Lippard, S. J., Binding of cis- and trans-dichlorodiammineplatinum(II) to DNA: evidence for unwinding and shortening of the double helix. *Science* **1979,** *203* (4384), 1014-6.

23. Krautbauer, R.; Clausen-Schaumann, H.; Gaub, H. E., Cisplatin changes the mechanics of single DNA molecules. *Angew. Chem. Int. Ed.* **2000,** *39* (21), 3912-3915.

24. Krautbauer, R.; Fischerlander, S.; Allen, S.; Gaub, H. E., Mechanical fingerprints of DNA drug complexes. *Single Mol.* **2002,** *3* (2-3), 97-103.

25. Howe-Grant, M.; Wu, K. C.; Bauer, W. R.; Lippard, S. J., Binding of platinum and palladium metallointercalation reagents and antitumor drugs to closed and open DNAs. *Biochemistry* **1976,** *15* (19), 4339-46.

26. Jennette, K.; Gill, J.; Sadownick, J.; Lippard, S. J., Metallointercalation reagents. Synthesis, characterization, and structural properties of thiolato (2, 2', 2''-terpyridine) platinum (II) complexes. *J Am Chem Soc* **1976,** *98* (20), 6159-6168.

27. Almaqwashi, A. A.; Andersson, J.; Lincoln, P.; Rouzina, I.; Westerlund, F.; Williams, M. C., DNA intercalation optimized by two-step molecular lock mechanism. *Sci Rep* **2016,** *6*, 37993.

28. Almaqwashi, A. A.; Andersson, J.; Lincoln, P.; Rouzina, I.; Westerlund, F.; Williams, M. C., Dissecting the Dynamic Pathways of Stereoselective DNA Threading Intercalation. *Biophys J* **2016,** *110* (6), 1255-63.

29. Almaqwashi, A. A.; Paramanathan, T.; Lincoln, P.; Rouzina, I.; Westerlund, F.; Williams, M. C., Strong DNA deformation required for extremely slow DNA threading intercalation by a binuclear ruthenium complex. *Nucleic Acids Res* **2014,** *42* (18), 11634-41.

30. Bahira, M.; McCauley, M. J.; Almaqwashi, A. A.; Lincoln, P.; Westerlund, F.; Rouzina, I.; Williams, M. C., A ruthenium dimer complex with a flexible linker slowly threads between DNA bases in two distinct steps. *Nucleic Acids Res* **2015,** *43* (18), 8856-67.

31. Luedtke, N. W.; Liu, Q.; Tor, Y., Synthesis, photophysical properties, and nucleic acid binding of phenanthridinium derivatives based on ethidium. *Bioorg Med Chem* **2003,** *11* (23), 5235-47.

32. Chua, E. Y.; Davey, G. E.; Chin, C. F.; Droge, P.; Ang, W. H.; Davey, C. A., Stereochemical control of nucleosome targeting by platinum-intercalator antitumor agents. *Nucleic Acids Res* **2015,** *43* (11), 5284-96.

33. Gregory, M. T.; Park, G. Y.; Johnstone, T. C.; Lee, Y. S.; Yang, W.; Lippard, S. J., Structural and mechanistic studies of polymerase eta bypass of phenanthriplatin DNA damage. *Proc Natl Acad Sci U S A* **2014,** *111* (25), 9133-8.

34. Riddell, I. A.; Johnstone, T. C.; Park, G. Y.; Lippard, S. J., Nucleotide Binding Preference of the Monofunctional Platinum Anticancer-Agent Phenanthriplatin. *Chem Eur J* **2016,** *22* (22), 7574-81.

TOC graphic